INSTITUTO SUPERIOR TÉCNICO

UNIVERSIDADE DE LISBOA

2nd Semester 2023/2024

Aerodynamics III

Shock tube's operation and Analysis of 2D/Axially Symmetric Minimum Length Nozzles (MLN)

GROUP NUMBER 4

Tiago Santos, 87290

João Gaspar, 96930

Guilherme Teixeira, 100210

Afonso Andrade, 108267

March 22, 2024

Contents

1 Introduction

On the scope of compressible fluid dynamics, this paper presents two studies that are fundamental aspects of the subject. Section 2 shows a shock tube study where some considerations on the operations are made including: flow proprieties, time discretization, gas varitions and geometry analysis. Also, in section 3 the design implications of a supersonic nozzle are explored, resorting to the method of characteristics in order to define the geometry of 2D planar and 2D axisymmetric minimum length nozzles.

2 Shock tube's operation

A shock tube, figure 1, is a device to produce a very high temperature and high velocity flow for a short period of time [1], which ables studies in a variaty of fields, such as chemical reactions, nuclear process and medical applications. Its main working principle is in the domain of compressible aerodynamics, where unsteady wave motion is a key aspect of study.

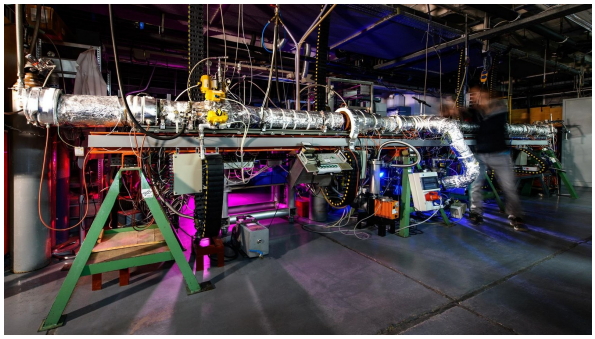

Figure 1: The shock tube facility operated by the German Aerospace Center (Deutsches Zentrum für Luft- und Raumfahrt; DLR) DLR-Institute of Combustion Technology, from `https://www.dlr.de/en/research-and-transfer/research-infrastructure/shock-tube-facility`

In this section, a shock tube design is conducted to understand the working principle and determine the main characteristics given certain postulated conditions. The shock tube is built considering two main sections: the driver and the driven sections, separated by a diaphragm (see Figure 2a). These two sections are filled with air (or another gas depending on the study). In this study other gases will be evaluated relative to their impact in shock wave mach number, with similar conditions of pressures p_1 and p_4. As the diaphragm breaks, the pressure difference generates a normal shock wave (see Figure 2b).

As the diaphragm breaks at time $t = 0$, the shock tube has two states, and this presents a Riemann problem, which consists of understanding how the air properties evolve over time [1]. The evolution of the tube's proprieties will evolve as the pressure discontinuity travells, by reference from image 2a, from left to right as a normal shock wave. On the other hand, a expansion wave propagates from right to left so the pressure on the driver section decreases. Another important aspect to take into consideration is a contact surface that separates the two regions as seen in figure 2b.

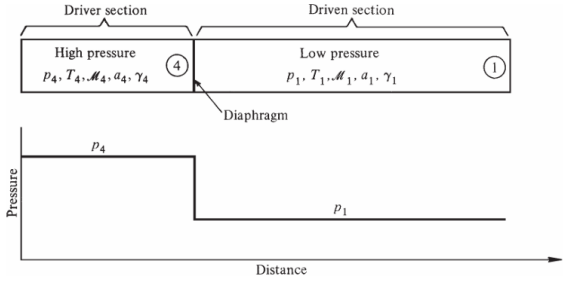

(a) Initial conditions in a pressure-driven shock tube.

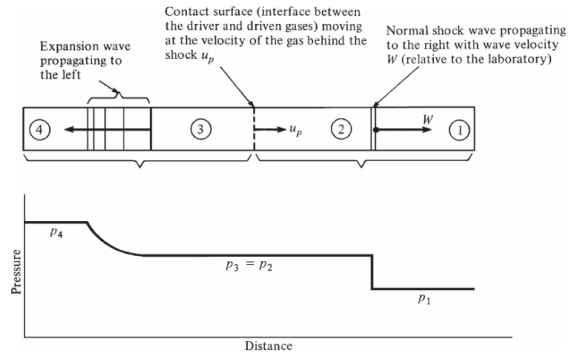

(b) Flow in a shock tube after the diaphragm is broken.

Figure 2: Scheme for the Shock tube design study, from [2]

2.1 Methodology

The main purpose of the present system is to perform aerodynamic tests on an object. There are different configurations of the fluids through this time-dependent process. Throughout this report, the region's definitions are coherent with Figure 3. In this Figure, one considers three situations. The Initial Condition is where the diaphragm is still present and there are two regions. Region 4 is called the driver section, with high pressure, and Region 1 (corresponding to the driven section) with lower pressure. The length of the driver and driven sections are set as L_4, and L_1, respectively. This fluid in these regions will always be stationary, with $u_1 = u_4 = 0$. When the diaphragm breaks several regions are formed and a moving shock (with speed M_s) toward Region 1 appears due to the

interaction between the two regions. Also, the contact surface between the two fluids will move (with speed U_p) in the same direction. The region between these two boundaries is set as Region 2. Also, after the removal of the diaphragm, an expansion wave will form that will allow for an isentropic lowering of pressure of region 4. The region comprised between the head and tail of the expansion wave will be set as Region 6, with head and tail velocities as v_f and v_m, respectively. Due to the movement of the contact surface, a region between the tail of the expansion wave and the contact surface will also be formed and here defined as Region 3. After the shock is reflected at the end of L_1 a new Region 5 is formed, and the pressure and temperature will severely increase, allowing for chemical reactions to take place.

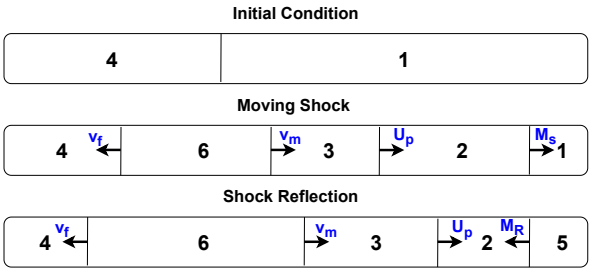

Figure 3: Regions definition throughout the report.

In Region 2 of Figure 3, a test subject may be placed and be subjected to a shock and then supersonic flow. The testing will occur in a time window that starts when the shock wave crosses the test subject and finishes when the shock wave, after reflection, intersects the test subject at the same time as the contact surface. This last description is the one that maximizes testing time by allowing the maximum time during operation.

The conditions present in the analysis are present in Table 1. L_1, p_1, T_1 and p_4 are present as inputs. Section 4 will be fed by a reservoir, isentropic and adiabatically, with pressure P_R and temperature T_R, until a pressure at the section of p_4. The main analysis will be performed until intersection of the shock wave with the contact surface and will use both fluids as air with $\gamma = 1.4$ and $R = 287.053 m^2/s^2/K$ [1]. Besides thermodynamic properties over time of the regions, L_4 will also be computed, assuming this value as the length that the head of the expansion wave travels until the end of the experiment, avoiding reflections and nontrivial computation zones.

The flowchart of the written code, whose equations and methodologies are discussed throughout this section, is present in the Appendix, at Figure 14.

Input						
Gas 1	**Gas 4**	**L1 [m]**	**P4 [kPa]**	**P1 [kPa]**	**PR [kPa]**	**T1 [K]**
Air	Air	4	30000	100	60000	300

Table 1: Inputs of the analysis.

2.1.1 Initial conditions

To determine the shock tube's proprieties during the experiment, all the initial conditions are necessary. From figure 2a, this means pressure,$p_{1,4}$, temperature $T_{1,4}$, mach number $M_{1,4}$, sound speed $a_{1,4}$ and specific heat capacity ratio $\gamma_{1,4}$. Although some variables are given, some considerations will be addressed.

First, the pressures and specific heat capacity ratio are already set in section 2.1. For the Mach number, $M_1 = M_4 = 0$ as the flow is considered stationary at $t \leq 0$. During the experiment, this remains constant, until shock wave reflection, leading to the elimination of region 1. For the calculation of sound speed, it can be directly computed by considering the initial temperatures and by using the next equation.

$$a = \sqrt{\gamma RT} \tag{1}$$

T_1 is given as problem input, however T_4 is an unknown conditon. To calculate T_4, by knowing that the feeding process from the reservoir is isentropic and adiabatic, Equation 2 is used and represents the isentropic relation for an ideal gas. By combining this equation with the ideal gas law (Equation 3) the driver section's temperature may be retrieved from 4. With this calculation, the $T_4 = 246.1K$, $a_1 = 347.2 m/s$ and $a_4 = 314.5 m/s$ are computed.

$$pv^{\gamma} = constant \tag{2}$$

$$pv = RT \tag{3}$$

$$T_4 = T_R \left(\frac{p_R}{p_4}\right)^{1/\gamma_4} \frac{p_4}{p_R} \tag{4}$$

2.1.2 Propagation and driver section length

A fundamental aspect of the shock tube, which deeply impacts the test duration, is the interactions of the normal shock wave and the contact surface, as previously mentioned. Since this time will dictate L_4 this section will present the aspects involved in propagating the position of the various physical mechanisms, computation of the driver section's length, and

thermodynamic properties retrieval.

To solve this question, the normal shock, the contact surface, and the expansion wave initial velocities should be computed. The normal shock wave velocity, W, can be determined by applying the conservation laws for mass balance, momentum, and energy. The equation used to compute the speed of the wave is presented in Equation 5. Before computing, it is necessary to calculate the pressure ratio across the shock wave $\frac{p2}{p1}$. This parameter may be estimated resorting to Equation 6, derived in [1], since all parameters are known.

$$W = a_1\sqrt{\frac{\gamma_1+1}{2\gamma_1}\left(\frac{p_2}{p_1}-1\right)+1} \tag{5}$$

$$\frac{p_4}{p_1} = \frac{p_2}{p_1}\left\{1-\frac{(\gamma_4-1)(a_1/a_4)(p_2/p_1-1)}{\sqrt{2\gamma_1\left[2\gamma_1+(\gamma_1+1)(p_2/p_1-1)\right]}}\right\}^{\frac{-2\gamma_4}{\gamma_4-1}} \tag{6}$$

After this step, the mach number of the shock wave can be computed by using equation 7.

$$M_s = \frac{W}{a_1} \tag{7}$$

From this result, one can estimate the Mach number of the shock wave after reflection, by employing Equation 8. To retrieve the speed of the reflected shock wave W_R, the speed of the contact surface (U_p) needs also to be retrieved since the need for this value is expressed in Equation 9, which presents the calculation of W_R. Also, a_2 is calculated using T_2, computed using the temperature relation due to the moving shock, present in Equation 10, and T_1. T_2 is then inputted in Equation 1.

$$\frac{M_R}{M_R^2-1} = \frac{M_s}{M_s^2-1}\sqrt{1+\frac{2(\gamma_1-1)}{(\gamma_1+1)^2}(M_s^2-1)\left(\gamma_1+\frac{1}{M_s^2}\right)} \tag{8}$$

$$W_R = M_R a_2 - U_p \tag{9}$$

$$T_2 = T_1\frac{p_2}{p_1}\left(\frac{\frac{\gamma_1+1}{\gamma_1-1}+\frac{p_2}{p_1}}{1+\frac{\gamma_1+1}{\gamma_1-1}\frac{p_2}{p_1}}\right) \tag{10}$$

For the contact surface speed, one can use the balance mass through the shock wave and apply the Rankine-Hugoniot relation to the computer its velocity, U_P, giving Equation 11.

$$U_p = \frac{a_1}{\gamma}\left(\frac{p_2}{p_1}-1\right)\left(\frac{\frac{2\gamma}{\gamma+1}}{\frac{p_2}{p_1}+\frac{\gamma-1}{\gamma+1}}\right)^{1/2} \tag{11}$$

Considering now the expansion wave, from Regions 3 to 4, there is a variation of density, ρ, pressure, p, and velocity, u. For the front and tail of the expansion wave, the wave characteristics associated are u_4-a_4 and u_3-a_3, respectively. Between these two waves, the Riemann invariants are kept constant.

$$u+\frac{2a}{\gamma-1} = constant \tag{12}$$

The wave velocity through the expansion wave is given by the following expression.

$$\frac{\mathrm{d}x}{\mathrm{d}t} = u-a \tag{13}$$

Thus the speed of the front and tail of the expansion wave is given by Equation 14 and 15 respectively.

$$v_f = -a_4 \tag{14}$$

$$v_m = u_3-a_3 \tag{15}$$

The v_f parameter can be known readily, however, further computations should be performed to compute v_m. First, one notes that the speed in Section 3 is the same as the contact surface, as given by equation 16. Also, the pressure of Section 3 will be the same of Section 2 (Equation 17). With the previous result for $\frac{p_2}{p_1}$ ratio, and by having access to p_1, p_2 and thus p_3 can be computed. With access to this variable, and by knowing that the expansion wave is isentropic, one can use the isentropic relation between Section 4 and 3 to estimate T_3 (Equation 18) and use this value to estimate a_3 (Equation 1), allowing for the calculation of v_m.

$$u_3 = u_2 = U_p \tag{16}$$

$$p_3 = p_2 \tag{17}$$

$$T_3 = T_4\left(\frac{p_3}{p_4}\right)^{\frac{\gamma_4-1}{\gamma_4}} \tag{18}$$

Finally, all velocities can be computed and the wave interactions can be determined. Figure 4 shows the wave's propagation position through the shock tube with time. The propagation method starts by integrating in time the position of the

shock wave, the contact surface, and the head and tail of the expansion wave. Note that the shock wave, after reaching the end of L_1 changes direction and speed, by the methodologies previously presented. After the computation of positions, the time at which the contact surface and shock wave intersect is computed. The position at which they intersect will lead to the location of the test subject, and indicate the time under operation, but also since the position of the head of the expansion is known at this time step, this position is taken as the value of L_4. To evaluate if the chosen time step is ideal, a time step refinement study is also performed, and presented in Section 2.2.1 of this report.

After having all the boundary definitions propagated through time, one can then define for each time step the regions based on the boundaries and thus calculate the properties for each position. Next, for each region, one will describe the process of computation. Note that the zero of the referential will be placed in the diaphragm location.

Region 4 is defined as being between $-L_4$ and the position of the head of the shock wave. In this region, as previously mentioned, the properties will correspond to p_4, T_4, a_4, $M_4 = 0$, and $u_4 = 0$. ρ_4 is computed using the ideal gas law.

Region 6 is defined as being between the head of the expansion wave and the tail of the expansion wave. In this region, one calculates first u_x, resorting to Equation 19. This value is used to calculate a_x, using Equation 20. This values allow to readily calculate the Mach number (u_x/a_x). Then, T_x and p_x are computed using Equations 21 and 22. The density is computed by using the ideal gas law.

$$u_x = \frac{2}{\gamma - 1}\left(a_4 + \frac{x}{t}\right) \tag{19}$$

$$\frac{a_x}{a_4} = 1 - \frac{\gamma - 1}{2}\left(\frac{u}{a_4}\right) \tag{20}$$

$$T_x = \frac{a_x^2}{R\gamma_4} \tag{21}$$

$$p_x = p_4\left(\frac{T_x}{T_4}\right)^{\frac{\gamma_4}{\gamma_4 - 1}} \tag{22}$$

Region 3 is defined as being between the tail of the expansion wave and the contact surface. In this region, as previously mentioned, the properties will correspond to p_3, T_3, a_3, $M_3 = u_3/a_3$, and u_3. ρ_3 is computed using the ideal gas law.

Region 2 is defined as being between the contact surface and the shock wave. In this region, as previously mentioned, the properties will correspond to p_2, T_2, a_2, $M_2 = u_2/a_2$, and u_2. ρ_2 is computed using the ideal gas law.

Wave		Velocity [m/s]	Mach
Normal shock wave	W	902.16	2.60
Reflected nomal shock wave	$W_{reflected}$	498.48	2.19
Expansion wave front	v_f	-314.49	
Expansion wave tail	v_m	454.04	
Contact Surface	U_p	640.44	

Table 2: Waves velocity

Region 1 is defined as being between the shock wave and the end of L_1, before the shock has been reflected. In this region, as previously mentioned, the properties will correspond to p_1, T_1, a_1, $M_1 = 0$, and $u_1 = 0$. ρ_1 is computed using the ideal gas law.

Region 5 is defined as being between the shock wave and the end of L_1, after the shock has been reflected. This region will experience an increase in thermodynamic properties such as temperature and pressure due to interaction with previously compressed gas. This can lead to chemical processes, in a region where the speed is still zero. Pressure and temperature in this region may be computed by Equation 23, and Equation 24 respectively. The speed of sound equation is used to calculate a_5 based on T_5. Since u_5 is zero, M_5 will also be zero. ρ_5 is computed using the ideal gas law.

$$\frac{p_5}{p_2} = 1 + \frac{2\gamma}{\gamma + 1}\left(M_R^2 - 1\right) \tag{23}$$

$$\frac{T_5}{T_2} = \left(1 + \frac{\gamma - 1}{2}M_R^2\right)\left(\frac{2\gamma}{\gamma - 1}M_R^2 - 1\right)\frac{2(\gamma - 1)}{M_R^2(\gamma + 1)^2} \tag{24}$$

The final property to be calculated is the entropy for each region. For each region, the initial conditions considered correspond to Section 4, which is defined as having zero value by this methodology. Expression 25 is used to calculate this parameter.

$$\Delta s = c_p ln\left(\frac{T_x}{T_4}\right) - Rln\left(\frac{p_x}{p_4}\right) \tag{25}$$

2.2 Results

As described in the methodology section, the first step to consider is to compute the waves velocoity right after the diaphragm rupture. Table 2 presents the initial velocities of the normal shock, W, the contact surface, U_p, the front, v_f, and tail, v_m, of the wave expansion, and also the normal shock wave velocity after the reflection on the right wall.

With the results on tabel 2, a $x-t$ diagram can me made. The simple velocity formula was used to compute the position of the wave over time. The key point here is to consider two important aspects. The algorithm should be able to find the wave-wall contact and change the normal shock wave velocity. Also, should find the instant when normal shock and contact surface interact and finish the execution. Figure 4 shows the resultant $x-t$ diagram with a time step of $\Delta t = 10^{-6}$. This value will be discussed in section 2.2.1.

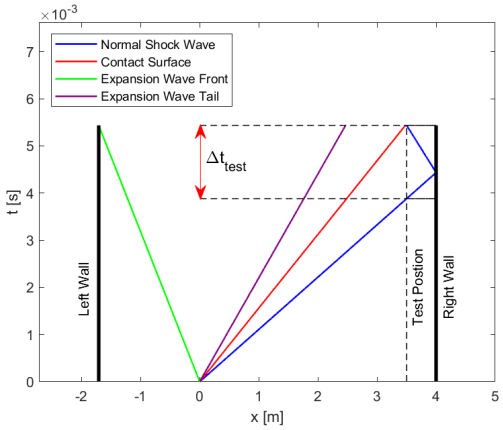

Figure 4: $x-t$ plot of the waves positions until the interactions of the normal shock wave and the contact surface

So, as a result from figure 4, some considerations and results can be obtained. Looking into the length of the driver section, the starting question of this section, the left wall was determined using the interaction time of the shock wave with the contact surface. The interaction time is $T_{inter} = 5.7ms$ meaning that the expansion front should touch the left wall for $t \geq 5.7ms$. This means that knowing the expansion wave front velocity the left wall should located at a minimum distance of $1.789m$ to the diaphragm, in other words, the driver's test section length should be at least $L_4 = 1.789m$.

Another important information that can be taken from the plot of figure 4 is the test position that is obtained considering the the period of time when no perturbation from waves happen. This time occurs when the normal shock wave passes the test object and the contact surface did not reach it. The experimental point is at $x_{exp} = 3.429m$. To maximise the test duration this position is given where the normal shock and the contact surface touch each other. So, the test interval starts at $t = 3.974ms$ after the diaphragm rupture and finishes at $t = 5.690ms$. This means that with the initial conditions it is possible to make experimental test during $\Delta t = 1.716ms$

As a final remark, the plot in figure 4 only shows what happens until the first wave-to-wave interaction. After that it is pointless to make further calculations because 1) after the interaction there is many possibilities for the resultant interaction; and 2) the test has already finished.

2.2.1 Time Step Analysis

As previously mentioned, in order to chose an adequate time step of the propagation of properties, an analysis of the time step used was performed. Due to capacity limitations in MATLAB, with a lower time step, the spatial discretization needs to be coarser. To have the maximum spacial discretization for visualization of results, a time step analysis was performed from 10^{-9} to 10^{-4} seconds. This allows to check how the position of test and L_4 would vary.

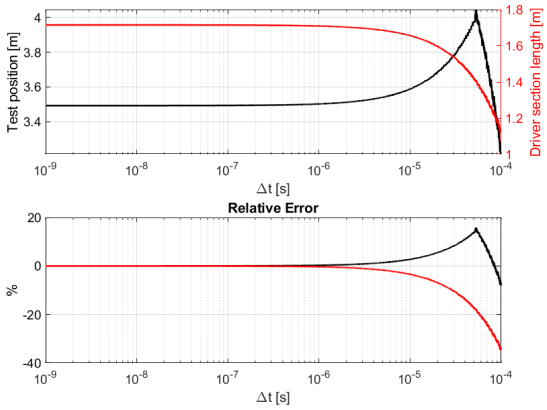

Figure 5: Convergency of test position, x_{exp}, with time step, Δt

Results are present in Figure 5. In the top plot, the values of each variable are plotted against the time step, and in the bottom plot the error, relative to the smaller time step is presented. It can be observed that when lowering the time step, the parameters eventually converge. After 10^{-6}, the error is very low and under 1%, and this is the time step chosen for the simulation. The error with larger time steps may be explained by the integration method. Since the computation of the position of the shock and expansion waves, and the contact surface is performed by integrating the speed in time, a too-large time-step causes larger displacements. For instance, in the case of the shock wave reflection, if the shock is near the end of L_1, the larger time-step would induce a larger displacement than the one allowable. So, when the shock crosses the threshold and the shock starts returning from the end of L_1, the time at the start of return will be higher. This, in turn, will influence the merging of the shock wave and the contact surface, since there were no cut-offs in the contact surface propagation. By performing this analysis, the time-step chosen

allows to reduce the error of the simulation, while allowing for faster computing times or larger spatial discretizations.

2.2.2 Proprieties over time

The shock tube's main importance is to adress different types of study as presented in section 2, this means that the controll of flow proprities is important. This section presents the results of flow proprieties over time for the entire shock tube length.

Using the algorithm presented in FIgure 14 it is possible to compute all proprieties from $t = 0ms$ until $t = 5.690ms$. However, figures 6 and 7 shows results for two time instants that are important. While figure 6 show the flow proprieties before the normal shock wave reflection, figure 7 shows the the flow proprieties after the reflection. This results are in according in theory, as can be see in figure 7.9, in [1].

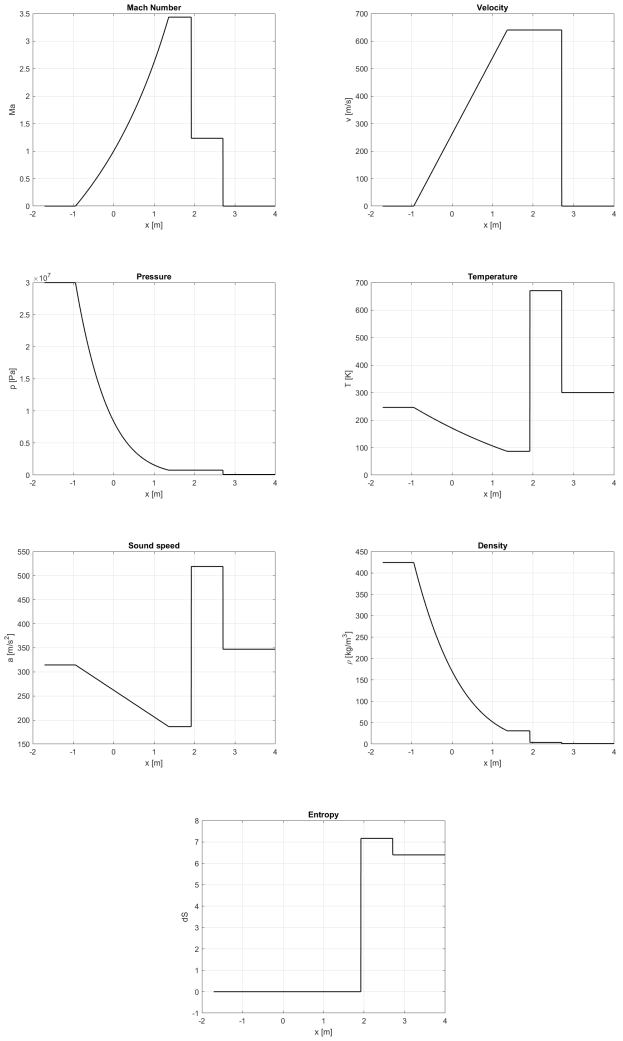

Figure 6: Flow proprieties at $t = 3ms$

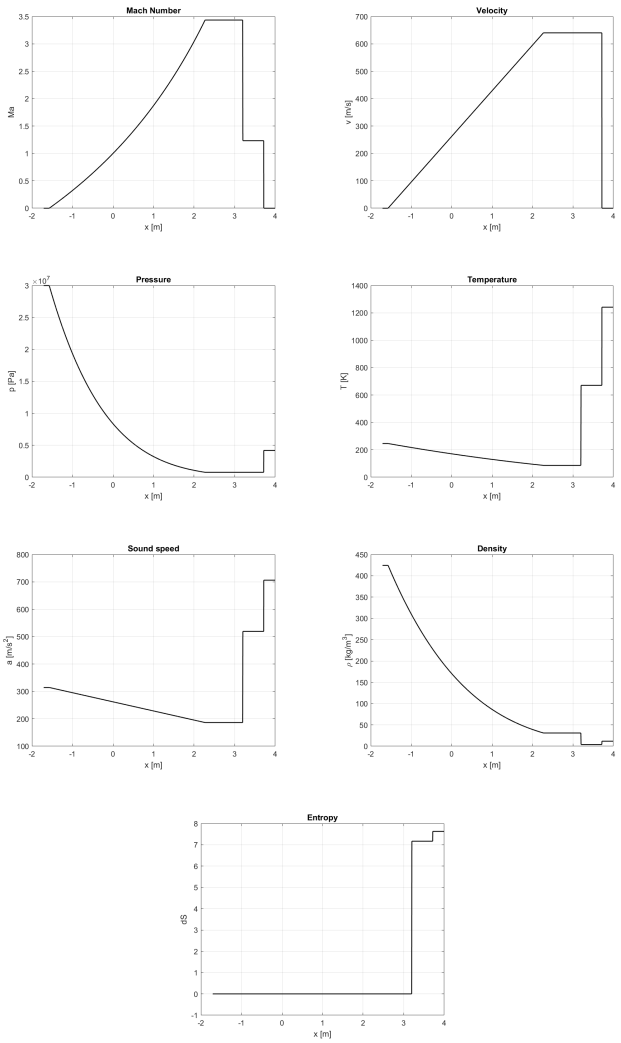

Figure 7: Flow proprieties at $t = 5ms$

A very interesting result for the proprieties that could be achieved considering the methodology adopted for the computational program, is a video with the flow changes with the time. Attached to the report, *flow_properties.mp4* file shows the complete variation of the flow proprieties from $t = 0ms$ until the end of the experience.

2.2.3 Flow proprieties variation at test postion

After having the time and spatial results of the properties along the shock tube, one can visualize the change of properties at the chosen x_{exp} location. Figure 8 presents the properties variation with time for that position. One may observe that properties correspond to the properties in Section 1 until $t = 3.974ms$. After this time, the shock wave passes through that position, and supersonic conditions present at the test position correspond to the ones of Section 2, until the end of the experiment at $t = 5.690ms$, when the reflected shock reaches

the position.

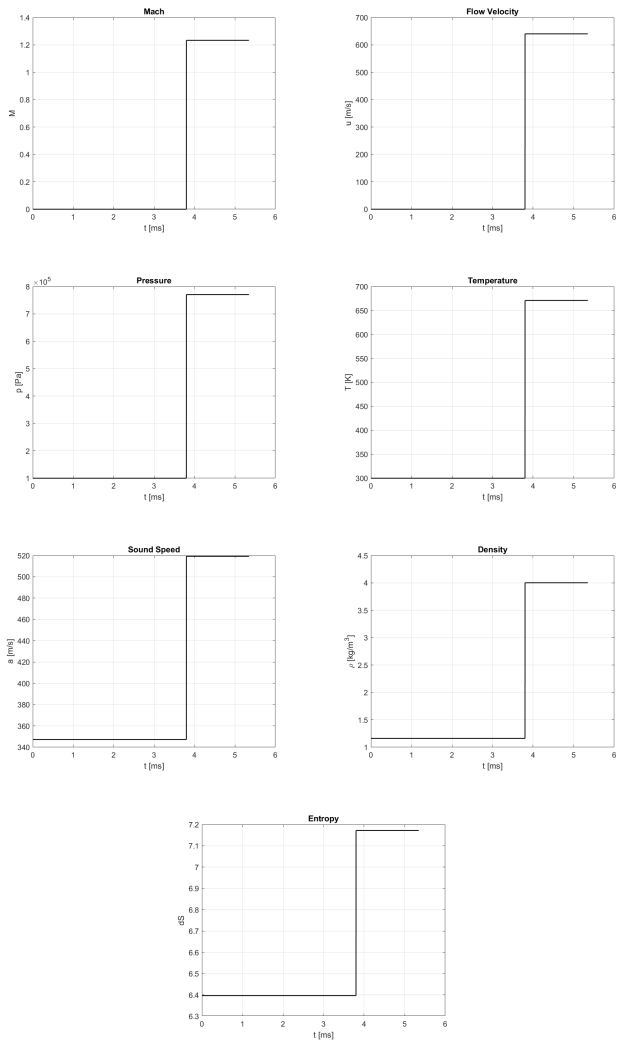

Figure 8: Flow proprieties at test position

2.2.4 Shock Mach number variation with gas choice

For the shock tube under the same conditions, one can maximize the Mach Number of the shock only by changing the gas on the driver and driven sections. From Equation 5, it can be observed that lower $a_1/a4$ ratios lead to higher p_2/p_1 ratios. This, in turn, will increase the shock wave speed W. If one considers also the lowering of a_1, coupled with the last statement, it is observed by Equation 7 that the Mach number of the shock increases. To lower a_1, a gas with high molecular mass $\mathscr{M}$ allows for a reduction of this value. To reduce a_1/a_4 ratio, a_4 should be the highest, so gases with lower $\mathscr{M}$ should be considered. So, choosing the lightest gas in the driver section and the heaviest in the driven section should increase the shock wave Mach number.

	Inputted Gases			
	Air	**Nitrogen**	**Helium**	**Hidrogen**
$\mathscr{M}$ [kg/kmol]	28.97	28	4	2
γ	1.4	1.4	1.66	1.41

Table 3: Gases considered in the analysis.

Shock Mach Number		**Driven Section Gas**			
		Air	**N2**	**He**	**H2**
Driver Section Gas	**Air**	2.60	2.57	1.61	1.42
	N2	2.62	2.60	1.62	1.43
	He	4.12	4.08	2.30	1.92
	H2	5.54	5.49	3.15	2.58

Table 4: Results for the shock Mach number for different gases.

To test this hypothesis, several gases are used and are combined between the driver and driven section. The gases considered, and specific properties are present in table 3.

Using the equations present in the methodology, the analysis results are present in Table 4. One observes that the higher Mach number is achieved for hydrogen at the driver section and air at the driven section. This confirms that Section 4 should have the lighter gas possible and Section 1 the heaviest. This result allows for testing the test subject at higher Mach numbers while maintaining air as the gas at the driven section. Although the higher values of the Mach number are in the hypersonic regime, the conclusions retrieved seem adequate.

2.2.5 Variation of driven section

Although the driven section length is defined in the problem statement, it is possible to study how to increase the test duration. Firstly, it is important to recap Figure 4 because it is important to understand how to increase the test duration. Directly, one can understand that the test duration is proportional to the normal shock wave and contact surface velocity and is influenced by the reflection normal shock wave.

Keeping the initial proprieties for driver and driven flow proprities, it is possible to increase test duration by increasing driven section length. Figure 9 shows how the test duration varies with the increase of the driven section length.

Once the proprieties are kept, it is possible to understand that the waves velocities are the same and then the test duration variation with the driven section length is linear. Meaning, the increase on the the driven section length increases the test duration.

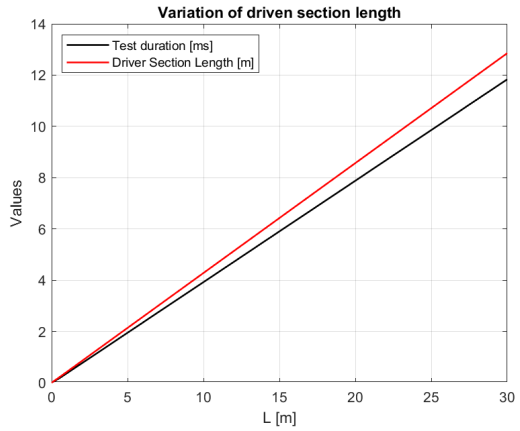

Figure 9: Test duration and driver section lenght variation with driven section length

However, by a consequence of the initial problem statement which says that the driver section should be so no expansion wave reflection occurs, 9 shows also the driver change with the driven section length. For the same reason as the test duration, the driver section length increases linearly.

As a final remark, it is important to say that no shear stress is considered on this study and boundary layer is not apply. For a shock tube with $30m$ length the boundary layers will have a huge impact on its performance, so further in-deep study should be adress to obtain better understanding in this sense.

3 Analysis of 2D and Axially Symmetric Minimum Length Nozzles (MLN)

3.1 Method of Characteristics

The method of characteristics is a numerical technique used in compressible aerodynamics to solve certain partial differential equations. It is particularly useful for solving problems involving shocks and expansion waves. The governing equations of fluid dynamics, describing conservation of mass, energy and momentum for a fluid flow, are non-linear and are difficult to solve analytically, especially when dealing with discontinuities in the flow, such as shocks. This method provides way to transform the original partial differential equations into ordinary differential equations along with characteristic curves, which represent the paths along information is propagated through the flow. By solving these simpler equations, flow properties along the characteristic curves can be calculated such as pressure, temperature, density or velocity.

3.2 Supersonic nozzle design

A supersonic nozzle features a convergent-divergent geometry, where it accelerates a fluid up to mach 1 at the throat and to supersonic velocities in the divergent section. The isentropic relations can be used to determine the area of the nozzle required for a desired exit mach number. However, the formation of shock waves makes this perspective not sufficient to have a proper nozzle design, in order to make sure shock waves will not be present within the nozzle the method of characteristics can be employed. There can be two ways of designing such nozzles: gently curved expansion sections, which produce very long nozzles, or minimum length nozzles, which are much shorter but result in a less refined approximation of the ideal geometry. Rocket engines are constrained in their length and mass, therefore their design follows the minimum nozzle length philosophy.

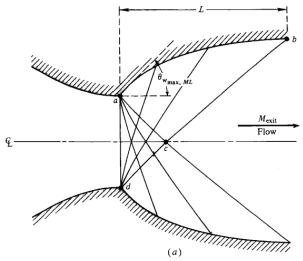

Figure 10: Schematic of minimum length nozzle

3.3 2D Planar Minimum length nozzle

As a part of this project the geometry of a 2D planar minimum length nozzle was determined using the method of characteristics. The known nozzle parameters are exit Mach number, 2, throat height, $1m$, gamma, 1.4, and number of characteristics, 3.

At the throat's corner (A), the first wall segment's $(4 \rightarrow 7)$ slope is defined as $\theta_{w,max}$, given by:

$\theta_{w,max} = \frac{\nu_{exit}}{2} = \frac{\nu(M_e)}{2} = \frac{\nu(2)}{2} = \frac{26.38}{2} = 13.19°$

The expansion fan coming out of this sharp corner was then subdivided by 3 characteristics, such that the first one is close to the sonic line at the throat. Ideally it should vertical and should correspond to the sonic line, however characteristics can only be defined for supersonic conditions. Therefore θ was set very close to 0º, having been arbitrarily set to the decimal part of $\theta_{w,max}$:

$\theta_1 = 0.19°$

The remaining angle was split by the two remaining characteristics:

$\theta_2 = \theta_1 + \frac{(\theta_{w,max} - \theta_1)}{2} = 0.19 + \frac{13}{2} = 6.69°$
$\theta_3 = \theta_2 + \frac{(\theta_{w,max} - \theta_1)}{2} = 6.69 + \frac{13}{2} = 13.19° = \theta_{w,max}$

3.3.1 Flow properties determination

1. Exit conditions (Points 8 and 9)

   From known exit conditions θ and Mach number can be inferred for points 8 and 9. These points are placed along a characteristic of a simple region, thus they share all the same flow properties:

   $M_8 = M_9 = M_e = 2.0$

   $\theta_8 = \theta_9 = 0°$

   Since two properties at these two points are known, it is possible to compute all others properties, namely:

   - Mach angle from Mach number:

   $$\mu = arcsin(\frac{1}{M}) \tag{26}$$

   - Prandtl-Meyer function from Mach number and γ:

   $\nu(M) = \sqrt{\frac{\gamma+1}{\gamma-1}} \cdot arctan(\sqrt{\frac{\gamma-1}{\gamma+1} \cdot (M^2-1)}) - arctan(\sqrt{M^2-1})$

   - The left and right-running characteristic's constants, from θ and $\nu(M)$:

   $$K_8^- = \theta_8 + \nu_8(M) = K_9^- \tag{27}$$

   $$K_8^+ = \theta_8 - \nu_8(M) = K_9^+ \tag{28}$$

2. Point 1,2 and 3

   From the division of the expansion fan the velocity orientation of the flow have already been defined for these points. In this region, $\theta = \nu(M)$ and so:

   $\nu_1 = \theta_1 = 0.19° \; \nu_2 = \theta_2 = 6.69° \; \nu_3 = \theta_3 = 13.19°$

   Since ν is a function of Mach number, it can be calculated for every point by solving equation **??** in order to M, yielding:

   $M_1 = 1.0264; M_2 = 1.3189; M_3 = 1.5435$

   As in the previous step, the mach angle and the characteristic's constants can be computed by 26 and 27,28, which completely defines their flow properties.

3. Point 5

   Point 5 is located on the centre line and so can be assumed to have its flow aligned with the x axis such that:

   $\theta_5 = 0°$

   The right running characteristic of point 2 is shared by point 5, therefore their constants are the same:

   $K_5^- = K_2^- = 13.38°$

   From:

   $K_5^- = \theta_5 + \nu_5$

   $\nu_5 = K_5^- = 13.38°$.

   Having determined two properties of the flow at this point, all others properties can be computed in the same manner as previous steps.

4. Point 6

   This particular point lies on a nonsimple region, therefore the only information known about it, is that it shares it's left running characteristic with point 5 and its right running characteristic with point 8:

   $K_6^+ = K_5^+ = -13.38° \; K_6^- = K_8^- = 26.38°$

   From these values, θ and ν can be obtained:

   $\theta_6 - \nu_6 = K_6^+ = -13.38° \; \theta_6 + \nu_6 = K_6^- = 26.38°$

   $\theta_6 = 6.5° \; \nu_6 = 19.88°$

   As they lie in a nonsimple region, their characteristics are actually curved and are approximated as straight lines.

5. Step 5 - Points 4 and 7

   Points 4 and 7 are located on the nozzle wall, and are in a simple region where no characteristics intersect, therefore all flow properties will be the same as with points 3 and 6 respectively, with which they share a characteristic line.

   - All flow properties in each point are resumed in table 12, located in the appendix

3.3.2 Point's coordinates determination

Having determined flow properties at very point, its is now possible to find the coordinates of each point, defining the nozzle's geometry. The nozzle's sharp corner (A) is defined as having coordinates [0;h_{throat}]=[0;1], and will be the starting point to determine other coordinates.

1. Point 1

   Point 1 is on the centre line and is connected to A by a characteristic with a known slope:

   $slope(C_1^-) = \theta_1 - \mu_1$

   $y_1 = 0$

   $x_1 = \tan(90 + slope(C_1^-) = \tan(90 + \theta_1 - \mu_1)$

2. Points 2,3,5,6 and 8

   These coordinates are defined as the intersection of two characteristics (2,3,6) or one characteristic and the centre line (5,8). Either way, the method to find it's coordinates is the same. The slope of a characteristic can be approximated to be a straight line (in reality, they are curved in this nonsimple region), with its slope being calculated as:

   $slope(C^+) = \frac{(\theta_1+\mu_1)+(\theta_2+\mu_2)}{2}$, for the example of the slope between points 1 and 2.

   Having determined the slopes of the characteristics that connect two points, coordinates can be computed by solving the system of equations (for the case of point 2):

   $\frac{y_2-y_A}{x_2-x_A} = \tan[slope(C^-)]$

   $\frac{y_2-y_1}{x_2-x_1} = \tan[slope(C^+)]$

   This process can then be repeated for the remaining points.

3. Points along the wall

   For points along the wall, we have the intersection of a characteristic in a simple region with the slope of a wall. The slope of the wall segments can be approximated to be the average of flow directions in the two points that define the segment:

   $slope_{wall} = \frac{\theta_i+\theta_f}{2}$

   Thus:

   $\theta_{w,1} = \frac{\theta_{w,max}+\theta_4}{2} = 13.19°$

   $\theta_{w,2} = \frac{\theta_4+\theta_7}{2} = 9.85°$

   $\theta_{w,3} = \frac{\theta_7+\theta_9}{2} = 3.25°$

   We can then employ the same methods as before to find the coordinates of the points along the wall.

   In particular, point 9's coordinates will define the nozzle's length and exit area:

   $L_{nozzle} = x_9 \quad A_{exit} = 2 \cdot y_9$

4. Coordinates Results

   From the results in table 5 it is possible to plot the nozzle´s geomtry presented in figure 11, where the 3 wall segments in red and 3 characteristics in blue can be seen.

Point	x (m)	y (m)
1	0.2313	0
2	0.4751	0.5628
3	0.5751	0.7045
4	0.9591	1.2248
5	1.1135	0
6	1.4214	0.2632
7	2.9266	1.5662
8	1.7913	0
9	4.6761	1.655

Table 5: Coordinate of all points in the nozzle

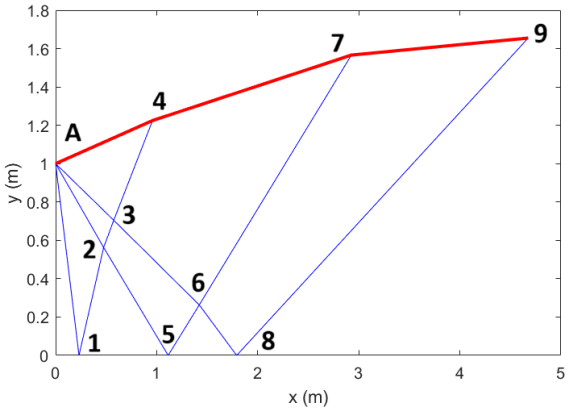

Figure 11: Nozzle geometry

3.4 Codes A and B results

In both codes A and B the number of characteristics is an input value. Since that, it is possible to vary that value and analyse the obtained results for nozzle exit area and length. For codes A and B the mach number at the exit is also an input, for code B the temperature and pressure work as inputs too.

From given T_0 and P_0 , with $\gamma = 1.4$ it is viabel to calculate temperature and pressures in the throat resorting to the following isentropic relations:

$$\frac{P^*}{P_0} = (1+\frac{\gamma-1}{2})^{\frac{-\gamma}{\gamma-1}} \tag{29}$$

$$\frac{T^*}{T_0} = (1+\frac{\gamma-1}{2})^{-1} \tag{30}$$

$$P^* = P_0 \cdot 0.5283 = 500 \cdot 0.5283 = 264.15KPa$$

$$T^* = T_0 * 0.833 = 400 \cdot 0.833 = 333.2K$$

In order to compare the results they can be plotted obtaining the following graphics:

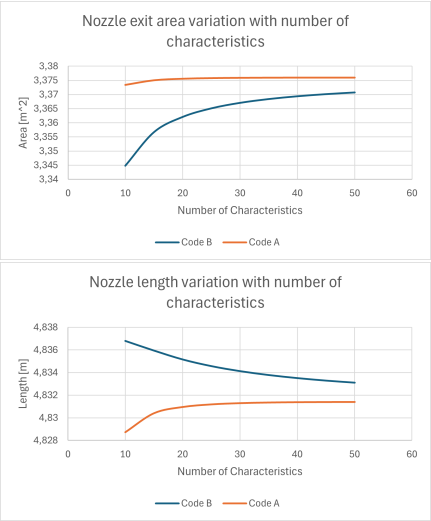

Figure 12: Area and Length results variation with characteristics number for both codes A and B

Interpreting these plots it is possible to conclude that growing the characteristics number in both codes, will lead to closer results. It is also notable that the number of characteristics has more influence on code B than on code A, the results variation is wider for code B.
In the following table are the isentropic and the code A and B results for 150 characteristics.

Isentropic	3.376 m^2
Code A	3.376 m^2
Code B	3.374 m^2

Table 7: Area results with different methods

Increasing the number of characteristics for 150 leads to much closer results and also closer to the isentropic ones. This turns possible to expect that for an infinity number of characteristic the results would converge to the same values.

3.5 Code D analysis

3.5.1 Influence of the different numerical parameters on the code D results

In order to evaluate the influence of each input variable on the code D, one at each time were varied and the results analyzed. The varied variables were the number of characteristics (N Length), compressed Kernel, and compression exponent. The following tables display the obtained results:

Compression Exponent	**Exit Area [m^2]**
3	2.5916
4	2.5940
5	2.5964
6	2.5906
7	2.5922

Table 8: Area results variation with different compression exponents

N Length	**Exit Area [m^2]**
10	2.5945
20	2.5964
30	2.5943
40	2.5966
50	2.5960

Table 9: Area results variation with different N length

Compressed Kernel	**Exit Area [m^2]**
1	2.5602
2	2.5826
3	2.5953
4	2.5961
5	2.5964

Table 10: Area results variation with different compressed Kernel

Analysing the results from tables 8 and 9 it is not possible to establish a correlation between the nozzle exit area and the

compression exponents or the number of characteristics. The results are oscillating and not following any pattern.
However, if the results for a variation on the compressed Kernel 10 were considered, an increase in the exit area occurs with the increase on the compressed Kernel.
By using kernel compression, more characteristics are inserted upstream of the first regular one. A greater degree of compression yields a more satisfactory result. This can be seen in 10, where high compression values of area converge to values to the closer to the isentropically determined exit area. One thing is common to all the results from code D, they are quite lower than the previous obtained ones either isentropically or through codes A and B.

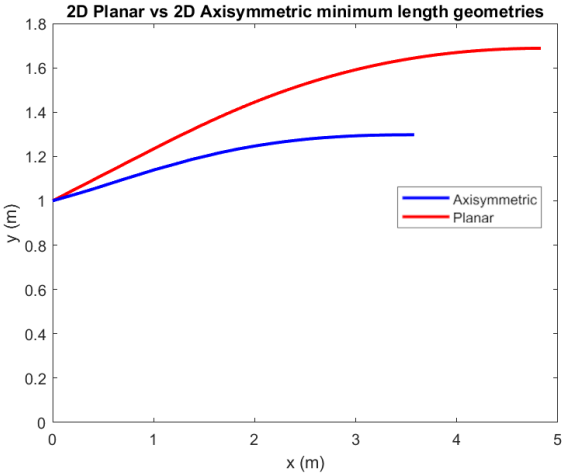

Figure 13: Comparison of planar and axisymmetric geometries

3.5.2 2D Axisymmetric nozzle design

To determine the nozzle geometry of a 2D axisymmetric nozzle, an algorithm, "Code D", was provided which was later analysed. When running "Code D", input mach number was iteratively adjusted to output the desired mach number ($M = 2$) in the last point of the nozzle, located at the exit. The overall functioning of this algorithm was resumed in a flow chart included in the appendix. 15

3.5.3 Initial overture angle

The initial maximum overture angle can be adjusted in "Code D", to obtain the required exit mach number at the exit, while maintaining input Mach number equal to 2. This angle was changed iteratively by reducing its value by small steps until exit mach was equal to the desired mach number.

This step is effectively the same as was done before, where input mach was adjusted to obtain desired mach at the exit, since in that case, initial overture angle was also changing beacuse it depends on input mach number: $\theta_{wmax,i} = \frac{\nu(M)}{4}$

3.5.4 Nozzle geometries comparison

By comparing the nozzle geometries obtained for the two types, it becomes apparent that an axisymmetric nozzle has less area and length when compared to a planar one for the same exit Mach number. The flow in an axisymmetric nozzle is expanded in both the radial and axial directions. This expansion allows the same amount of mass flow to achieve the desired exit Mach number with a smaller cross-sectional area compared to a planar nozzle, where expansion only occurs in the axial direction. As a result, the axisymmetric design allows for more efficient nozzle geometry, reducing the overall size and weight of the nozzle.

Bibliography

[1] J. C. F. Pereira, *Aerodinâmica Compressível*. Instituto Superior Técnico: AEIST, 2021, vol. 1.

[2] J. D. Anderson, *Modern compressible flow: with historical perspective*, en, Fourth edition. New York, NY: McGraw Hill, 2021, ISBN: 978-1-260-57082-3.

Appendix

A Flowchart Shock tube

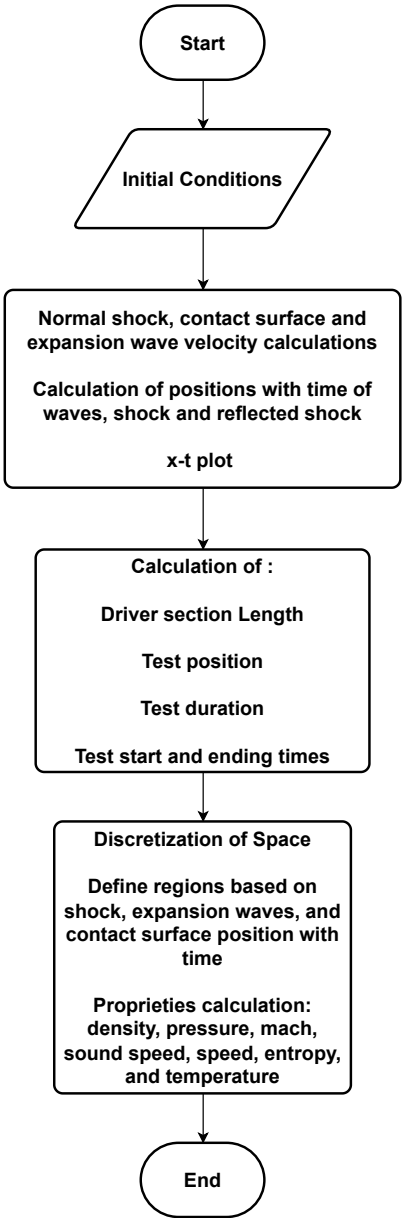

Figure 14: Flowchart of shock tube analysis main code.

B Flow properties at the points of the 2D planar nozzle

Node	K-	K+	θ	Prandtl (ν)	Mach	μ	obs.
1	0,38	0,00	0,19	0,19	1,0264	76,98	
2	13,38	0,00	6,69	6,69	1,3189	49,31	
3	26,38	0,00	13,19	13,19	1,5435	40,38	
4	26,38	0,00	13,19	13,19	1,5435	40,38	same as 3
5	13,38	-13,38	0,00	13,38	1,5500	40,18	
6	26,38	-13,38	6,50	19,88	1,7708	34,38	
7	26,38	-13,38	6,50	19,88	1,7708	34,38	same as 6
8	26,38	-26,38	0,00	26,38	2,0000	30,00	
9	26,38	-26,38	0,00	26,38	2,0000	30,00	same as 8
	inferred values						
	given values						
	computed values						

Table 12: Flow properties

C Flowchart of "code D"

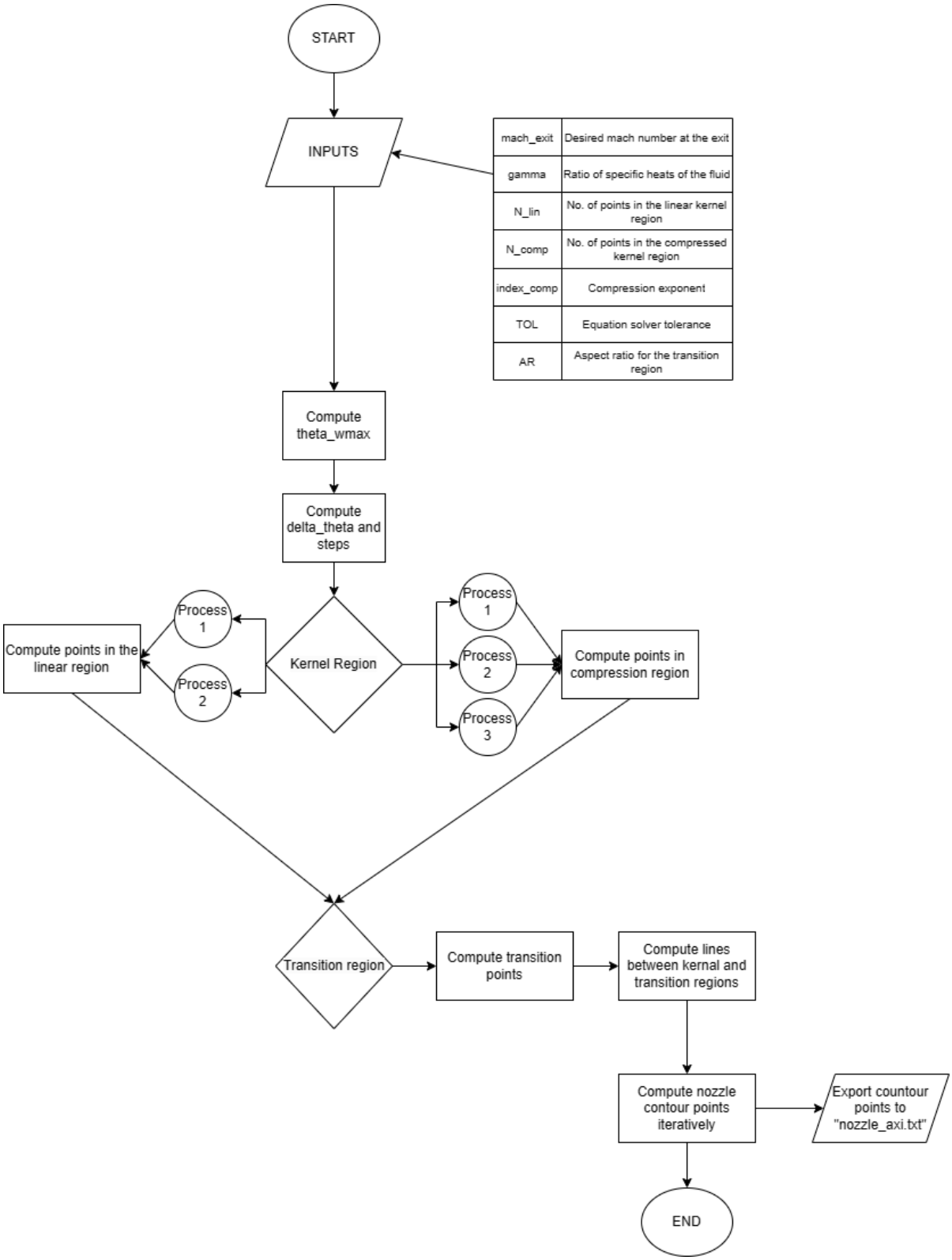

Figure 15: Code D Flow Chart

D Code B results for 25 characteristics

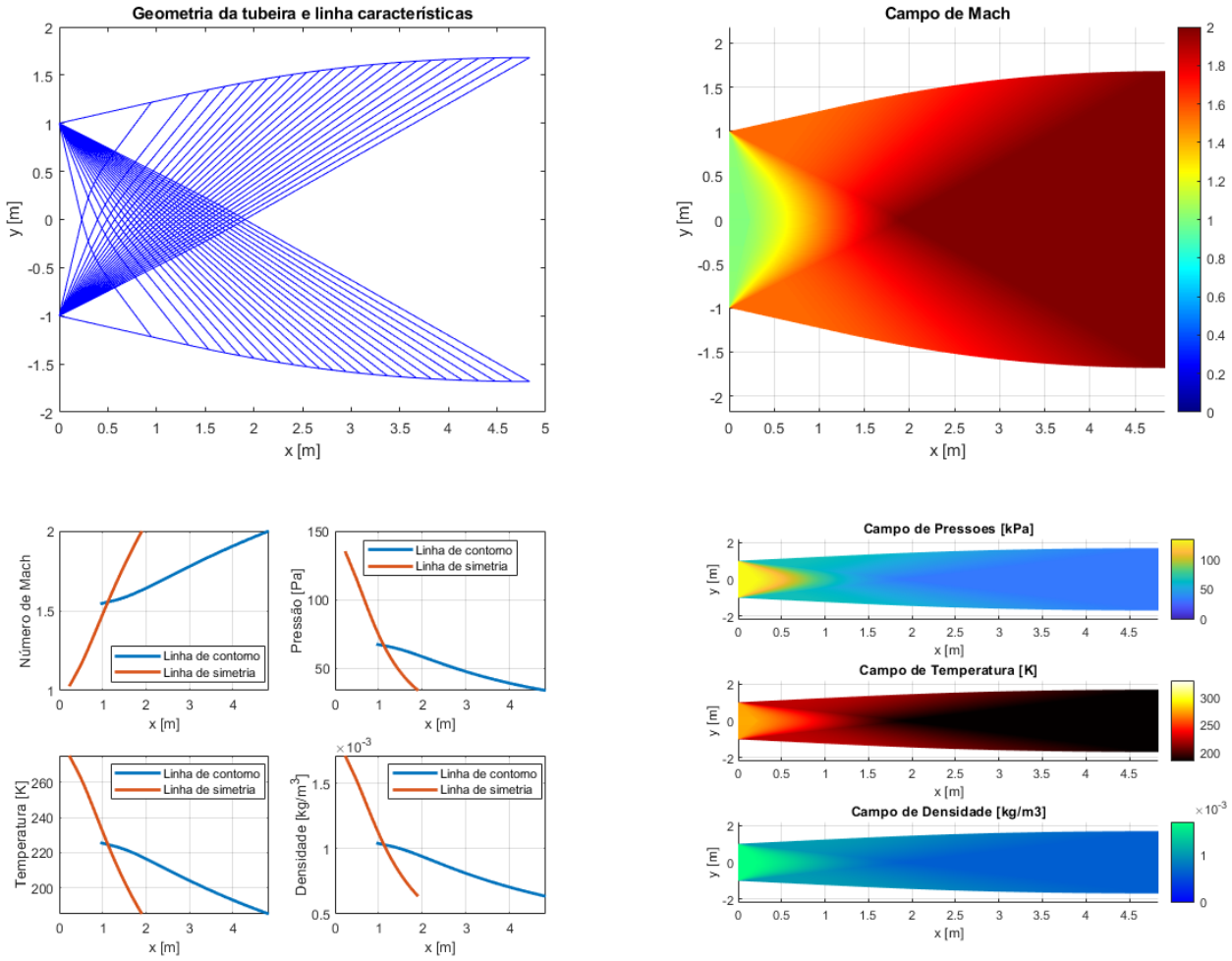

Figure 16: Code B results for 25 characteristics